Published in final edited form as:
*Int J Electrochem Sci*. 2014 February ; 9(2): 890–900.

# Comparison of the 2D and 3D Nanostructured Lectin-Based Biosensors for *In Situ* Detection of Sialic Acid on Glycoproteins

**Tomas Bertok**, **Alena Sediva**, **Alica Vikartovska**, and **Jan Tkac***

Department of glycobiotechnology, Institute of chemistry, Center for glycomics, Slovak academy of sciences, Dubravska cesta 9, Bratislava 845 38, Slovak republic

## Abstract

We present here comparison of a build-up of two ultrasensitive lectin biosensors based on 2D or 3D architecture. A 2D lectin biosensor was prepared by a covalent immobilisation of lectin *Sambucus nigra* agglutinin (SNA) recognising sialic acid directly on a mixed self-assembled monolayer (SAM) on planar gold surfaces. A 3D biosensor was prepared by covalent immobilisation of SNA lectin on a mixed SAM layer formed on gold nanoparticles. Surface plasmon resonance technique allowed to follow kinetics of a mixed SAM (1:1 mixture of 11-mercaptoundecanoic acid and 6-mercaptohexanol) formation on a bare gold electrode and on an electrode modified by 5 nm and 20 nm gold nanoparticles (AuNPs). Results from the study revealed that a mixed SAM formation is slower on surfaces with increased curvature, the process of SAM formation on all surfaces is completed within 6 min, but a density of thiols on such surfaces differs significantly. Quartz crystal microbalance experiments showed that a surface density of immobilised lectin of (2.53 ± 0.01) pmol $cm^{-2}$ was higher on planar gold surface compared to the surface modified by 20 nm AuNPs with a surface density of (0.94 ± 0.01) pmol $cm^{-2}$. Even though a larger amount of SNA lectin was immobilised on a surface of the 2D biosensor compared to the 3D biosensor, lectin molecules immobilised on AuNPs were more accessible for its analytes – glycoproteins fetuin and asialofetuin, containing different amount of sialic acid on the protein surface. Most likely a better accessibility of lectin for its analytes on a 3D surface and proper interfacial properties of a 3D surface are behind unprecedented detection limit down to aM level for the lectin biosensor based on such a nanoscale tuned interface.

### Keywords

biosensor; *Sambucus nigra* lectin; electrochemical impedance spectroscopy (EIS); glycoproteins; gold nanoparticles

## 1 Introduction

The irreplaceable role of glycans is already well known in many physiological and pathological processes, such as cell adhesion and growth, signalling and communication, maturation of erythrocytes, viral infection, immune response, disease progress and many others[1]. As a part of glycoproteins, glycans influence folding, stability, molecular

* ian.tkac@savba.sk.


Europe PMC Funders Author Manuscripts

interactions, resistance against proteases and in the case of enzymes also their activity[2]. Because of a combinatory potential of these molecules, glycans carry information (termed as a sugar code) about the parental biomolecule or cell function they are a part of. Glycoproteomics, the study of a glycome attached to protein molecules, became an important branch of the ′-omics′ family, since it became apparent that the modulation of the protein function is affected by changes on the protein backbone rather than only by a gene regulation[3,4]. Moreover, it is estimated that more than 50% of all eukaryotic proteins are glycosylated[5] and more than 70% of all protein based therapeutics are glycoproteins[6,7]. However, analysis of the glycan structure by instrumental techniques such as capillary electrophoresis, liquid chromatography and mass spectrometry often requires releasing a glycan chain from a glycoprotein and analysis is quite complex[8].

Lectins are naturally occurring glycan decipherers with a weak affinity and a low specificity for a particular analyte[9]. Thus, a relatively small array of lectins can be sufficient for glycoprofiling of samples in a highly efficient way without a need for a glycan release[10]. Traditional lectin-based techniques[11] including an ELISA-like detection platform[12] are time-consuming, requiring a high analyte concentration, a labelling step or providing only qualitative results. Recently introduced a state-of-the-art lectin microarray platform of detection revealed that *in situ* glycoprofiling in a highly parallel manner is possible, but this technique has some drawbacks such as a high detection limit and requirement to use labels[13,14], thus novel sensing platforms addressing these issues are most welcome[8,15]. An initial effort in this direction for a label-free and *in situ* glycoprofiling was recently launched by Joshi's group, an approach based on electrochemical impedance spectroscopy (EIS) with lectins immobilised on a gold printed circuit microelectrode array[16]. EIS is a highly sensitive technique based on the electric perturbation of a thin layer on a conductive material[1] and EIS-based lectin biosensors are considered to be the most promising glycoprofiling tool[15]. Our recent contributions in this field showed that glycoproteins can be detected down to fM or aM level[17,18].

Several forms of sialic acid terminated glycans have a prominent role in many pathological processes, such as chronic inflammation, HIV and influenza infection and cancer, and thus *in-situ* detection of sialic acid on glycoproteins in biological samples is of a great interest for the medical diagnostics[19,20]. Removal of a single molecule of sialic acid from glycan of an antibody (IgG) may change its activity from being an anti-inflammatory into a pro-inflammatory agent[21]. Thus, a lectin biosensor developed for a robust analysis of sialic acid composition may be applied in many different fields. In this short communication we would like to compare sensitivity of previously described the 2D and the 3D lectin biosensors for sialic acid assays on glycoproteins[17,18] with a focus on molecular organisation of interfacial layers of the 2D and the 3D biosensors.

## 2 Experimental Part

### 2.1 Materials

11-mercaptoundecanoic acid (MUA), 6-mercaptohexanol (MH), potassium hexacyanoferrate(III), potassium hexacyanoferrate(II) trihydrate, potassium chloride, N-hydroxysuccinimide (NHS), N-(3-dimethylaminopropyl)-N′-ethylcarbodiimide

hydrochloride (EDC), poly(vinylalcohol) (PVA, Mowiol® 4-88), sodium periodate, ethylene glycol, acetonitrile, fetuin (FET, 8.7% of sialic acid), asialofetuin (ASF, ≤ 0.5% of sialic acid) and gold nanoparticles (AuNPs, 5 and 20 nm diameter) were purchased from Sigma Aldrich (St. Louis, USA, www.sigmaaldrich.com). SNA lectin from *Sambucus nigra* was purchased from Gentaur (Kampenhout, Belgium, www.gentaur.com). 11-aminoundecanethiol hydrochloride was purchased from Dojindo (Germany). Ethanol for UV/VIS spectroscopy (ultra pure) was purchased from Slavus (Bratislava, Slovakia, www.slavus.sk). Zeba™ spin desalting columns (40k MWCO) for protein purification were purchased from Thermo Scientific. All buffer components were dissolved in ultra pure deionised and filtered water (DW).

## 2.2 Electrode pre-treatment and preparation of the 2D and the 3D biosensors

Planar polycrystalline gold electrodes with a diameter of 1.6 mm (Bioanalytical systems, USA) were cleaned for the next experiments by a reductive desorption, mechanical polishing, piranha treatment, electrochemical polishing and stripping of gold oxide as described previously[22,23]. Electrochemical procedures were run on a laboratory potentiostat/galvanostat Autolab PGSTAT 128N (Ecochemie, Netherlands) in a measuring cell containing Ag/AgCl reference and a counter platinum electrode (both from Bioanalytical systems, USA). Electrochemical polishing was employed for calculation of a surface area of bare gold electrode or a gold electrode modified by gold nanoparticles by integration of a gold reductive peak as shown previously[18]**Error! Bookmark not defined.**.

A 2D biosensor interface was formed on a mixed SAM on bare gold electrode prepared by incubation of 1:1 mixture of 1 mM ethanolic solutions of MUA and MH in a dark for 1 h. Subsequently, carboxyl groups of MUA were activated by 1:1 mixture of 200 mM EDC and 50 mM NHS for 15 min, washed and the electrode was further modified by immobilisation of lectins from a 10 μM stock solution in a 50 mM phosphate buffer solution (PBS, pH 6.5) for 20 min in an inverted position. Finally, the surface was blocked by incubation of electrodes in 2.5% PVA in DW, prepared in 80 °C DW and cooled down to 20 °C prior incubation, for 30 min.

A 3D biosensor was constructed by formation of the 1$^{st}$ SAM layer on a bare gold electrode from 1 mM ethanolic solution of 11-aminoundecanethiol incubated in a dark overnight. Such layer worked as a linker for attachment of 5 nm or 20 nm AuNPs (in the form as obtained from a provider), which were incubated with modified gold electrode in an inverted position overnight. A mixed 2$^{nd}$ SAM was prepared on the AuNPs modified polycrystalline gold electrode from a 1:1 mixture of 1 mM MUA and 1 mM MH, both in dissolved ethanol, by incubation in the dark for 60 min. The surface was washed by absolute EtOH and DW. Finally the lectin was covalently linked to the modified electrode via amine coupling using EDC/NHS coupling chemistry and the surface was blocked by PVA, as described previously.

## 2.3 Chemical oxidation of glycoproteins

ASF glycan structure was chemically oxidised by sodium periodate as described previously[7]. Shortly, 10 μM stock solution of ASF was oxidised by 10 mM sodium

Europe PMC Funders Author Manuscripts

periodate in 50% acetonitrile for 2 h in a dark. The reaction was stopped by addition of ethyleneglycol to a final concentration of 15% (v/v) and incubated for 1 h in a dark. Further, free aldehyde groups formed during the glycan oxidation were blocked by addition of 1 mM ethanolamine. The mixture was incubated for 1 h in a dark and finally the oxidised ASF (oxASF) was recovered by a repeated centrifugation in a desalting column and the protein was stored at -20 °C in aliquots.

### 2.4 Electrochemical impedance spectroscopy (EIS) measurements

The EIS measurements were performed in an electrolyte containing 5 mM potassium hexacyanoferrate(III), 5 mM potassium hexacyanoferrate(II) and 100 mM KCl. The electrolyte was freshly prepared before the measurement and filtered with a 0.2 μm sterile filters to remove any impurities. The EIS measurements were run at 50 different frequencies (ranging from 0.1 Hz up to 100 kHz) under Nova Software 1.8 and 1.9, respectively (Ecochemie, Netherlands). Data acquired were evaluated using the same software represented by a Nyquist plot with a circuit R(C[RW]) employed for data fitting.

### 2.5 Quartz crystal microbalance (QCM) measurements

All QCM measurements were performed with a laboratory potentiostat/galvanostat Autolab PGSTAT 128N (Ecochemie, Netherlands) equipment using an optional EQCM module. The changes of a mass were evaluated using Sauerbrey's equation:

$$\Delta f = -\frac{2f_0^2}{A\sqrt{\rho_q \mu_q}}.\Delta m \quad (1)$$

where Δf is the frequency change (Hz), $f_0$ is the nominal resonant frequency of the quartz crystal (6 MHz), Δm is the change in mass ($g.cm^{-2}$) and $\mu_q$ is a shear modulus of a quartz ($g.cm^{-1}.s^{-2}$), A is the surface area and $\rho_q$ is a density of quartz in $g.ml^{-1}$. For a 6 MHz crystal, the whole equation can be simplified to:

$$\Delta f = -C_f.\Delta m$$

where $C_f$ is a frequency constant 0.0815 $Hz.ng^{-1}.cm^2$. The measurements were run at ambient temperature and monitored and evaluated using the Nova 1.9 software.

### 2.6 Surface Plasmon resonance (SPR) assays

For the SPR measurements, a gold chip (Litcon, Sweden) of 12x12x0.3 mm was used. The chip was modified with HS-$C_{11}$-$NH_2$ and subsequently with 5 nm and 20 nm AuNPs outside SPR machine (see section *Gold electrode pre-treatment and SAM formation*) and subsequently inserted into SPR machine (SR7000DC, Reichert, USA) operated with an autosampler. First, EtOH for UV/VIS was injected for a few minutes until a stable signal was obtained and then formation of a mixed SAM was monitored by injection of 1 mM solution of alkanethiols (1:1 MUA and MH) for 15 min. The sensorgram was recorded and

evaluated using SPR Autolink software 1.1.7 (Reichert, USA) and for calculation of the total amount of thiols adsorbed, density of thiols was taken into account as described previously[24].

## 3 Results and Discussion

A schematic representation, drawn to scale, of an interfacial layer of the 2D and the 3D biosensor is shown in Fig. 1. While for the 2D biosensor, lectin is immobilised on a 1$^{st}$ mixed SAM layer directly deposited on a gold surface, the 3D biosensor configuration is constructed from various layers (Fig. 1). The main function of the 1$^{st}$ SAM layer composed of 11-aminoundecanethiol deposited on gold electrode for the 3D biosensor is to attach AuNPs. The 2$^{nd}$ mixed SAM layer is then formed on AuNPs for covalent immobilisation of the lectin.

### 3.1 A surface area of bare and AuNPs modified electrodes

In order to calculate a bare planar gold surface area and a surface area of gold nanoparticles after deposition on a bare planar gold surface, an electrochemical procedure was applied as previously described[22]. Calculation of gold surface area was based on quantification of gold oxide reduced upon a cathodic sweep during electrochemical oxidation and reduction of gold.

Bare gold electrode has a surface area of (0.024 ± 0.003) cm$^2$, what gives a roughness factor of 1.2, consistent with our previous study[18]. The electrochemical surface area of gold nanoparticle modified electrodes was much higher (0.033-0.052 cm$^2$) compared to bare gold electrode and in order to calculate only contribution of AuNPs these values were subtracted from a value of electrochemical surface area of a bare planar gold (Fig. 2).

### 3.2 A mixed SAM formation

Although reductive desorption can be applied for quantification of a surface density of thiols on gold surfaces[22], it works quite well for single component SAMs and in many cases the surface coverage can be overestimated due to presence of oxygen in the electrolyte during measurements. The main reason why we applied surface plasmon resonance (SPR) for quantification of the surface density of thiols within a mixed SAM is a high robustness and sensitivity of the device to quantify the amount of thiols attached[25,26]. Moreover, SPR technique can provide information about kinetics of thiol adsorption (i.e. $t_{1/2}$, what is a time needed to form a thiol layer equivalent to 50% of a full monolayer). From Fig. 3 and Table 1 it can be concluded that formation of a mixed SAM is much faster process on bare gold electrode, when compared to formation of a mixed SAM on AuNP modified surfaces. Generally it can be said, that formation of a mixed SAM layer is a very quick process and thiol adsorption is completed within 6 min. An equilibrium SPR signal from a fitting procedure was used for calculation of a surface density of a mixed thiol layer, taking into account the ratio of MUA:MH of 1:1 on the surface is the same as in the solution as can be seen in Table 1. Moreover, in the case of surfaces modified by AuNPs only the surface of nanoparticles was taken into account for calculation of a surface density of thiols on their surfaces.

A surface density of thiols on 5 nm AuNPs is very low (Table 1), what can be ascribed to a dense population of 5 nm AuNPs on the surface with a nanoparticle separation of only 2.0 nm, calculated from a surface density for 5 nm AuNPs as described in our previous paper[18]. This gap between nanoparticles is too small to accommodate MUA chains with a length of 1.9-2.1 nm[24], what results in nanoparticles not fully covered by thiols. Separation between neighbouring nanoparticles attached on surfaces for 20 nm AuNPs was calculated to be 31 nm from a surface density of 0.073 pmol $cm^{-2}$ obtained previously from SEM images[18]. Thus, this gap between 20 nm nanoparticles is large enough allowing to fully cover nanoparticles by thiols. From Table 1 it can be seen that a calculated surface coverage on 20 nm AuNPs is $(4.347 \pm 0.005)^* 10^{14}$ thiols $cm^{-2}$, a value in a good agreement with a value of $(4.97 \pm 0.01)^* 10^{14}$ MUA thiols $cm^{-2}$, observed on smaller 13 nm AuNPs[27].

### 3.3 Lectin immobilisation

Since the best performance of the 3D lectin biosensor was observed on a surface modified by 20 nm AuNPs[18], the 3-D biosensor based on this configuration is here compared to the 2D biosensor configuration. Quartz crystal microbalance (QCM) was applied for quantification of SNA lectin immobilised on both surfaces (Fig. 4), revealing a surface coverage of $(2.53 \pm 0.01)$ pmol $cm^{-2}$ for the 2D configuration and $(0.94 \pm 0.01)$ pmol $cm^{-2}$ for the 3D configuration. Surface coverage of SNA immobilised on 2D surface obtained from a QCM experiment is consistent with a value of 1.9 pmol $cm^{-2}$ previously read from SPR data for the same lectin on the same surface[18]. When an amount of SNA lectin attached to the 3D interface was re-calculated per surface area of AuNPs a surface density of $(2.60 \pm 0.03)$ pmol $cm^{-2}$ could be obtained. Such value is comparable to the value obtained on 2D modified gold, suggesting that in case of a 3D interface fabricated from 20 nm AuNPs, separation between nanoparticles allow immobilisation of SNA lectin all over the nanoparticle surface (Fig. 1).

### 3.4 The 2D biosensor vs. the 3D biosensor

In the final part of the manuscript a comparison of the response to the main analyte fetuin (FET) very close to the detection limit for 2D and 3D configuration is shown (Fig. 5), underlining ultrasensitive performance of the 3D biosensor to detect its analyte down to aM level.

Finally, a comparison between sensitivity of the 2D biosensor vs. 3D biosensor is done taking into account the absolute amount of lectin in fmoles (fmol) immobilised on the surface of gold electrode (Fig. 6). These results really indicate that while a lower amount of lectin of 0.94 pmol $cm^{-2}$ was immobilised on the 3D biosensor surface, compared to the 2D biosensor surface (2.53 pmol $cm^{-2}$), a sensitivity of fetuin detection relative to the lectin immobilised was $(205 \pm 9)$ Ω $decade^{-1}$ $fmol^{-1}$ for the 3D biosensor and $(127 \pm 3)$ Ω $decade^{-1}$ $fmol^{-1}$ for the 2D biosensor. A similar story was true for another analyte asialofetuin (ASF, Fig. 6). These results suggest lectin immobilised on 20 nm AuNPs is more accessible for interaction with its analytes compared to lectin immobilised directly on a bare gold electrode.

## 4 Conclusions

The present study was aimed to better understand interfacial properties of layers formed on 2D or 3D gold surfaces. Results of the study showed kinetics of a mixed SAM formation and its surface density differ significantly on three surfaces tested, but the process of SAM formation on all surfaces was quite quick with completion of SAMs within 6 min. The 3D lectin biosensor offered not only a better accessibility for its glycoprotein analytes, but most importantly a higher sensitivity of detection and a much lower detection limit compared to the 2D lectin biosensor (≈1 aM vs. ≈1 fM). The results suggest that the nanostructured lectin biosensors have a great potential to be employed in early biomedical diagnostics of diseases such as arthritis or cancer, which are connected to aberrant glycosylation of protein biomarkers in biological fluids.

## Acknowledgements

The financial support from the Slovak research and development agency APVV 0282-11 and from VEGA 2/0127/10 is acknowledged. The research leading to these results has received funding from the European Research Council under the European Union's Seventh Framework Programme (FP/2007–2013)/ERC Grant Agreement n. 311532.

## References

1. Bertok T, Katrlik J, Gemeiner P, Tkac J. Microchim Acta. 2013; 180:1.
2. Oliveira C, Teixiera JA, Domingues L. Crit Rev Biotechnol. 2013; 33:66. [PubMed: 22530774]
3. Smith DF, Cummings R. Mol Cell Proteomics. 2013; 12:902. [PubMed: 23412570]
4. Zauner G, Selman MHJ, Bondt A, Rombouts Y, Blank D, Deelder AM, Wuhrer M. Mol Cell Proteomics. 2013; 12:856. [PubMed: 23325769]
5. Baker JL, Celik E, DeLisa MP. Trends Biotechnol. 2013; 31:313. [PubMed: 23582719]
6. Beck A, Reichert JM. mAbs. 2012; 4:419. [PubMed: 22699226]
7. Li Y, Tian Y, Rezai T, Prakash A, Lopez MF, Chan DW, Zhang H. Anal Chem. 2011; 83:240. [PubMed: 21141837]
8. Reuel NF, Mu B, Zhang J, Hinckley A, Strano MS. Chem Soc Rev. 2012; 41:5744. [PubMed: 22868627]
9. Gabius H-J, Andre S, Jimenez-Barbero J, Romero A, Solis D. Trends Biochem Sci. 2011; 36:298. [PubMed: 21458998]
10. Arnaud J, Audfray A, Imberty A. Chem Soc Rev. 2013; 42:4798. [PubMed: 23353569]
11. Mislovicova D, Gemeiner P, Kozarova A, Kozar T. Biologia. 2009; 64:1.
12. Mislovicova D, Katrlik J, Paulovicova E, Gemeiner P, Tkac J. Colloids Surf, B-Biointerf. 2012; 94:163.
13. Gemeiner P, Mislovicova D, Tkac J, Svitel J, Patoprsty V, Hrabarova E, Kogan G, Kozar T. Biotechnol Adv. 2009; 27:1. [PubMed: 18703130]
14. Katrlik J, Svitel J, Gemeiner P, Kozar T, Tkac J. Med Res Rev. 2010; 30:394. [PubMed: 20099267]
15. Tkac, J.; Bertok, T.; Nahalka, J.; Gemeiner, P. Perspectives in glycomics and lectin engineering. LECTINS; Laboratory Protocol Series, Methods in Molecular Biology. Hirabayashi, J., editor. Humana Press/Springer; in press
16. La Belle JT, Gerlach JQ, Svarovsky S, Joshi L. Anal Chem. 2007; 79:6959. [PubMed: 17658764]
17. Bertok T, Gemeiner P, Mikula M, Gemeiner P, Tkac J. Microchim Acta. 2013; 180:151.
18. Bertok T, Sediva A, Katrlik J, Gemeiner P, Mikula M, Nosko M, Tkac J. Talanta. 2013; 108:11. [PubMed: 23601864]
19. Chen X, Varki A. ACS Chemical Biology. 2010; 5:163. [PubMed: 20020717]

20. Kim J-H, Resende R, Wennekes T, Chen H-M, Bance N, Buchini S, Watts AG, Pilling P, Streltsov VA, Petric M, Liggins R, et al. Science. 2013; 340:71. [PubMed: 23429702]
21. Anthony RM, Kobayashi T, Wermeling F, Ravetch JV. Nature. 2011; 475:110. [PubMed: 21685887]
22. Tkac J, Davis JJ. J Electroanal Chem. 2008; 621:117.
23. Bertok T, Klukova L, Sediva A, Kasak P, Semak V, Micusik M, Omastova M, Chovanova L, Vlcek M, Imrich R, Vikartovska A, et al. Anal Chem. 2013; 85:7324. [PubMed: 23808876]
24. Balasubramanian S, Revzin A, Simonian A. Electroanalysis. 2006; 18:1885.
25. Davis JJ, Tkac J, Laurenson S, Ferrigno PK. Anal Chem. 2007; 79:1089. [PubMed: 17263340]
26. Davis JJ, Tkac J, Humphreys R, Buxton AT, Lee TA, Ferrigno PK. Anal Chem. 2009; 81:3314. [PubMed: 19320493]
27. Ivanov, MR. Covalently functionalized gold nanoparticles: synthesis, characterization, and integration into capillary electrophoresis. PhD. thesis; University of Iowa: 2011.


Europe PMC Funders Author Manuscripts

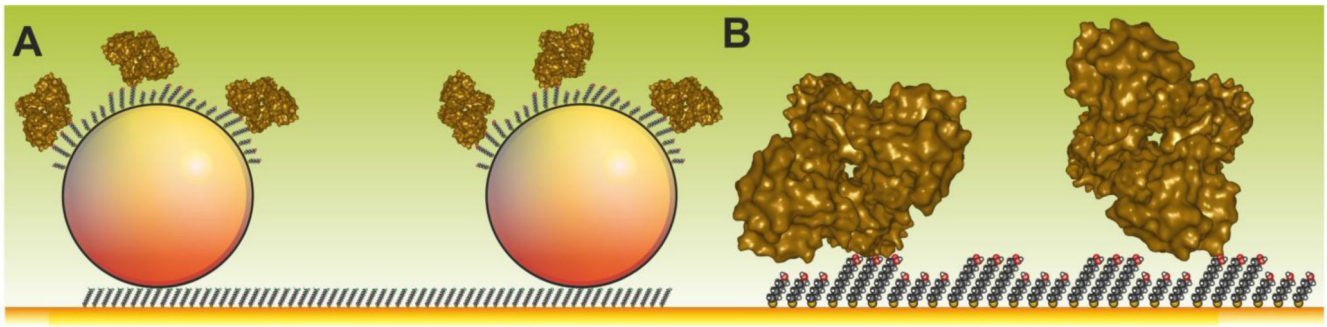


**Figure 1.**

A graphical representation drawn to scale of interfacial layers applied to build up the 3D biosensor based on integrated 20 nm gold nanoparticles (A) or the 2D biosensor (B). The 3D biosensor was build up on a planar gold surface by chemisorptions of 11-aminoundekanethiol, functioning as a linker for attachment of 20 nm gold nanoparticles, represented in a form of a sphere. On every gold nanoparticle a mixed SAM composed of 11-mercaptoundecanoic acid (MUA) and 6-mercaptohexanol (MH) was formed for covalent immobilisation of lectin (A). The 2D biosensor was formed by incubation of a planar gold with MUA and MH for covalent attachment of a lectin.

Europe PMC Funders Author Manuscripts

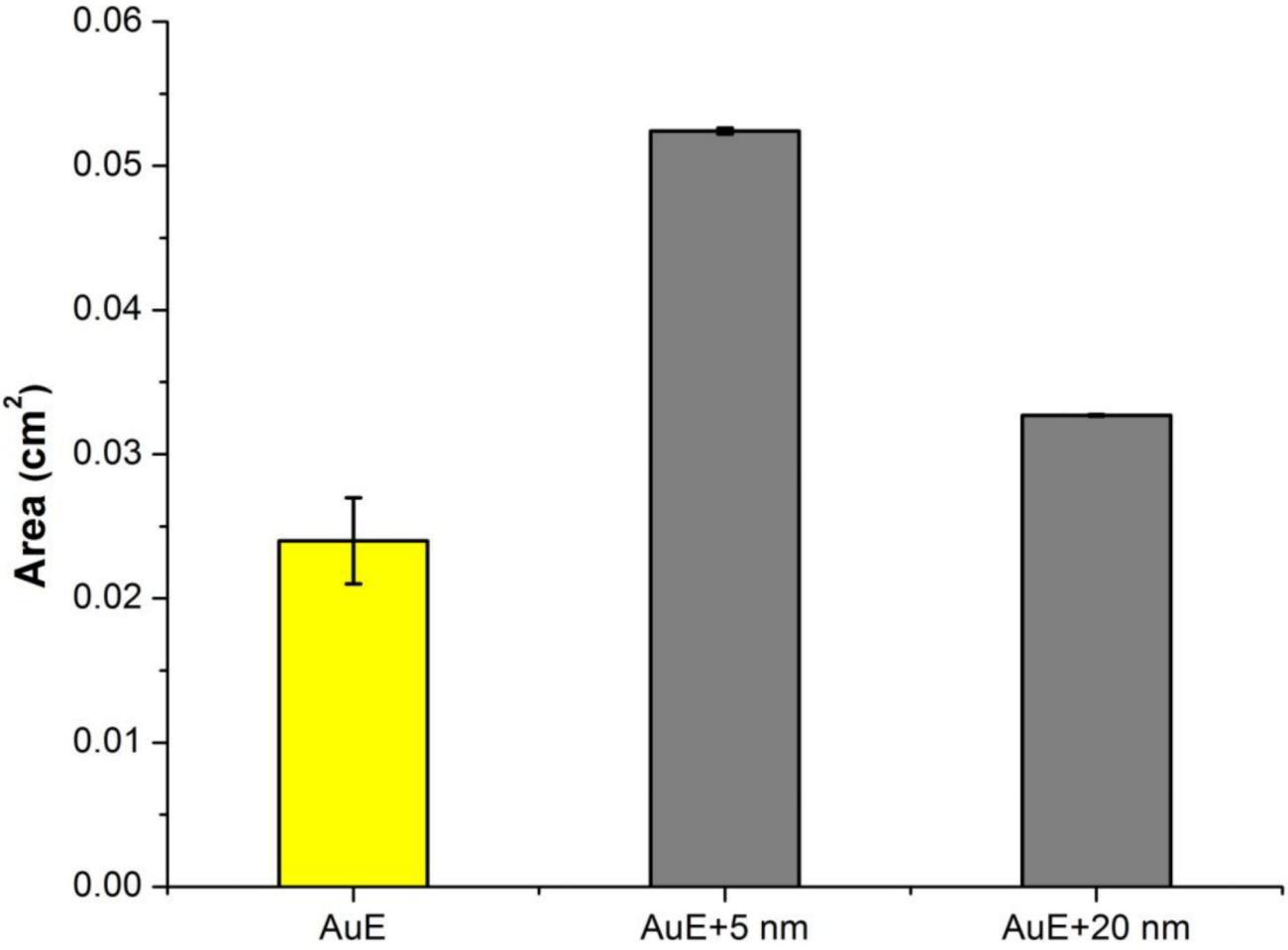


**Figure 2.**

Electrochemical gold surface area of a planar gold electrode before (AuE, yellow) and after modification by gold nanoparticles of two different sizes (5 and 20 nm). All measurements were done at least in triplicate.

Europe PMC Funders Author Manuscripts

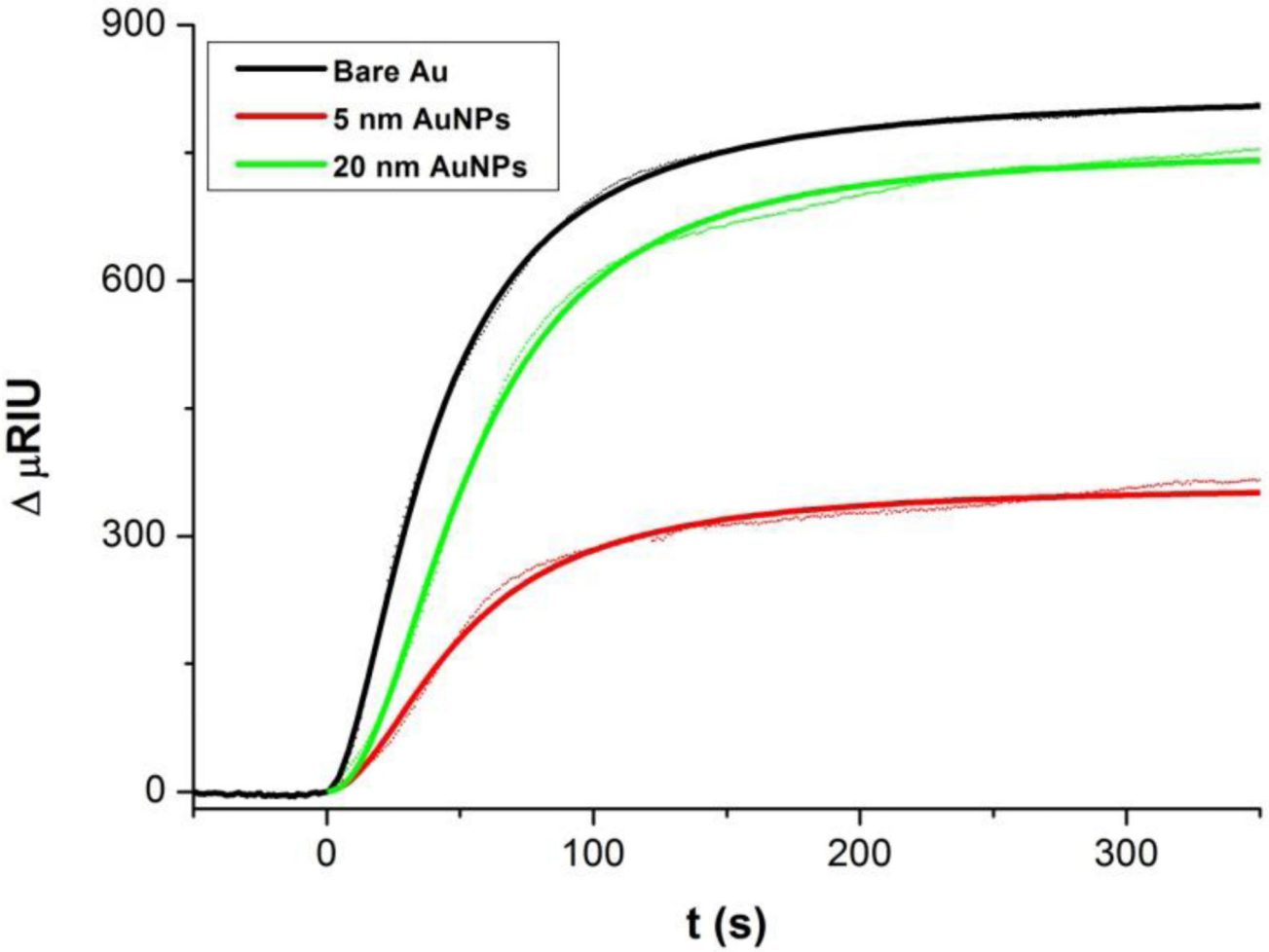


**Figure 3.**

SPR sensorgram showing formation of a mixed SAM from 1:1 solution of MUA and MH on three different surfaces. The association phase represented by raw data as a thin layer was fitted by a Hill plot (thick line) in order to obtained kinetic constants of the adsorption process (i.e. $t_{1/2}$ and equilibrium surface coverage $\Gamma_e$).

Europe PMC Funders Author Manuscripts

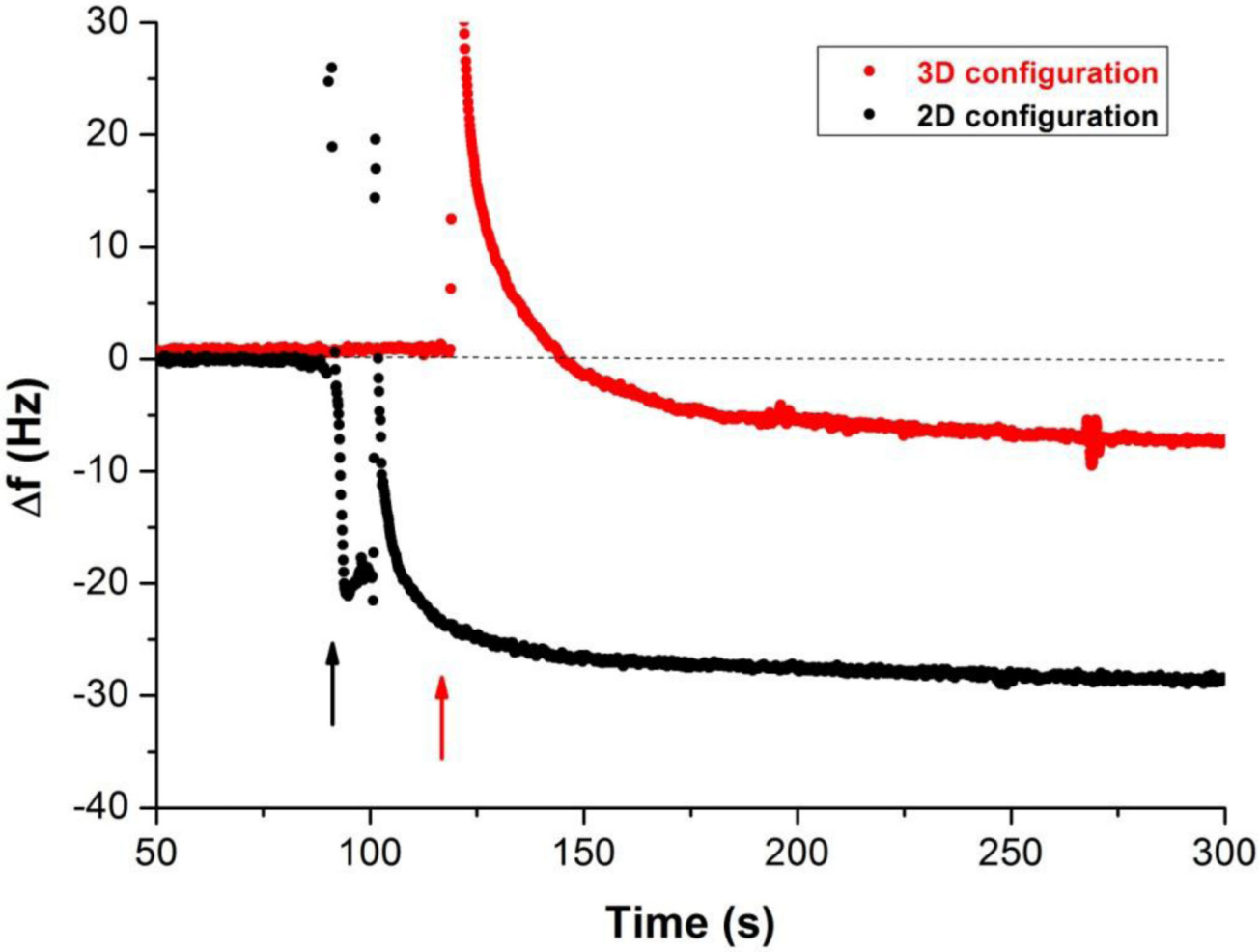


**Figure 4.**
Injection of SNA lectin (indicated by arrows) on a 2D and a 3D surface during immobilisation probed by QCM.

Europe PMC Funders Author Manuscripts

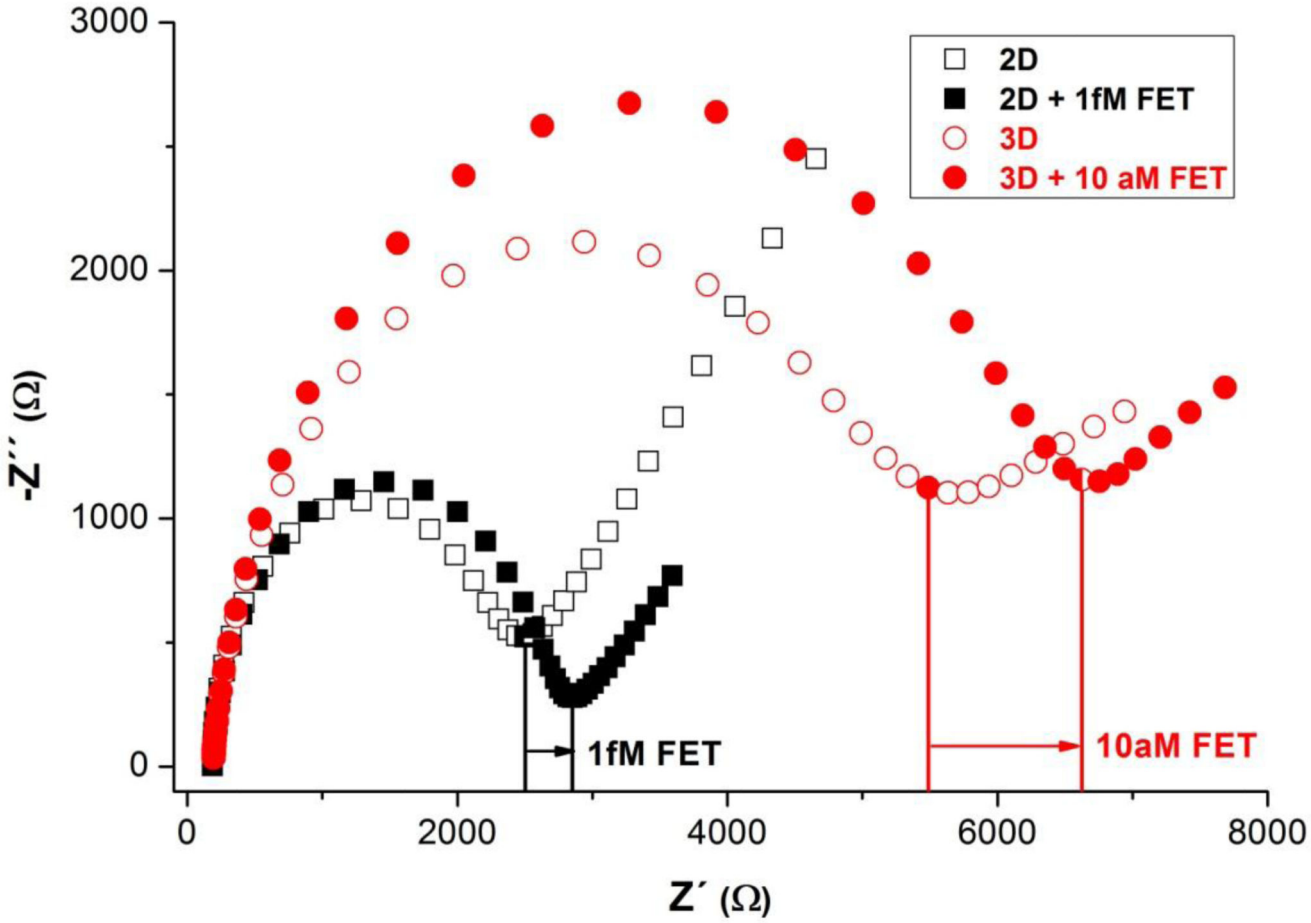


**Figure 5.**
Comparison of the response of the 2D and the 3D biosensor to its analyte fetuin (FET) with concentration close to the detection limit, represented in a Nyquist plot.

Europe PMC Funders Author Manuscripts

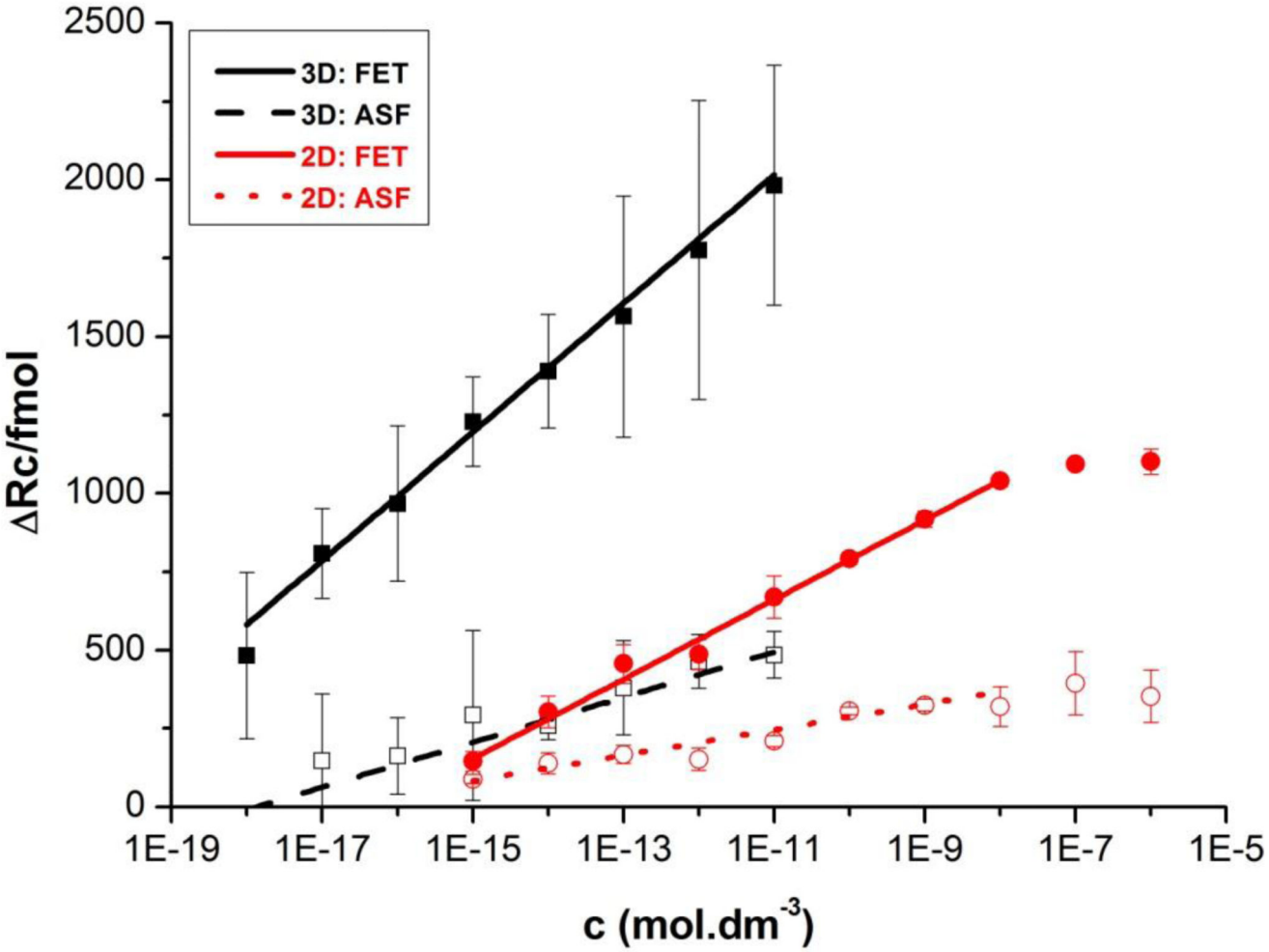


**Figure 6.**

Comparison of calibration curves for the 2D and the 3D lectin biosensor towards its two analytes – glycoproteins fetuin (FET) and asialofetuin (ASF).

Europe PMC Funders Author Manuscripts

**Table 1**

Results of SPR signal fitting by a Hill plot during formation of a mixed SAM layer on various surfaces.

| Modification | $t_{1/2}$(s) | Equilibrium SPR signal (Δμ RIU) | $10^{-14}*\Gamma_S$ (molecules $cm^{-2}$) |
|---|---|---|---|
| Bare Au | 39.1 ± 0.1 | 821 ± 1 | 1.712 ± 0.002 |
| 5 nm AuNPs | 56.0 ± 0.4 | 356 ± 1 | 0.627 ± 0.002 |
| 20 nm AuNPs | 53.4 ± 0.2 | 755 ± 1 | 4.347 ± 0.005 |

$t_{1/2}$ - a time needed to form a thiol layer equivalent to 50% of a full monolayer, $\Gamma_e$ – surface coverage at equilibrium